

Silencing of AEBP1 inhibits proliferation and promotes apoptosis via the AKT signaling pathway in osteosarcoma

CUNFENG JIA, ZHEN GONG and LEI ZHANG

Department of Spinal Surgery, Zhangqiu District People's Hospital, Jinan, Shandong 250200, P.R. China

Received December 29, 2024; Accepted May 8, 2025

DOI: 10.3892/br.2025.2006

Abstract. Adipocyte enhancer-binding protein 1 (AEBP1) has emerged as a novel regulator in the tumorigenic progression of various cancers. Despite its significance, the expression and functions of AEBP1 in osteosarcoma (OS) remain largely unexplored. The GEO database was used to screen for novel targets of osteosarcoma and AEBP1 was focused on since its expression and functions in OS remain to be thoroughly elucidated. Thus, the aim of the present study was to investigate the potential biological functions of AEBP1 in OS. UALCAN and CCLE databases were then used to analyze the expression levels of AEBP1. By employing siRNA, AEBP1 was silenced in human OS cells and the expression of AEBP1 at the mRNA and protein levels was assessed through reverse transcription-quantitative PCR and western blot analysis, respectively. Subsequently, the effects of AEBP1 silencing on the proliferation and apoptosis of human OS cell lines were investigated using MTT, 5-ethynyl-2'-deoxyuridine, clone formation, flow cytometry and TUNEL assays. The results revealed that silencing of AEBP1 inhibited OS cell proliferation, promoted apoptosis, and induced G₁ cell cycle arrest in U2OS cells. Mechanistically, AEBP1 was found to be highly expressed in sarcoma and OS cell lines. Silencing of AEBP1 suppressed the expression of p-AKT and cyclin D1, regulating OS cell proliferation. Furthermore, it reduced the expression levels of Bcl-2, while promoting Bax expression, thereby enhancing OS cell apoptosis. Notably, the silencing of AEBP1 counteracted the activation of the AKT signaling pathway induced by an activator. In conclusion, the findings of the present study indicated that silencing of AEBP1 suppressed OS proliferation, revealing AEBP1 as a promising therapeutic target for OS treatment.

Introduction

Osteosarcoma (OS) is recognized as the most prevalent primary bone malignancy, considered to stem from bone-forming mesenchymal stem cells. The pathogenesis of OS hinges significantly on the aberrant activation of oncogenes and the inactivation of tumor suppressor genes, which occurs through somatic mutations and epigenetic mechanisms (1). Worldwide, the estimated annual incidence of OS exceeds 2 million cases, with a primary peak occurring at ages 15-19 years (incidence, 8-11 million/year) and a minor peak occurring at >60 years of age (2,3). OS predominantly affects the metaphysis of long extremity bones, such as the distal femur, proximal tibia, proximal femur, and proximal humerus, with rare occurrences in the axial skeleton and other sites (4). Although the combination of surgery and chemotherapy has significantly improved outcomes for patients with OS, the prognosis for metastatic or recurrent OS remains unsatisfactory (5). Thus, the identification of novel targeted drugs and therapeutic targets is an urgent priority.

Initially, adipocyte enhancer-binding protein 1 (AEBP1) was identified as a transcriptional repressor of the adipose P2 (aP2) gene in preadipocytes (6), and its expression is down-regulated during the progress of adipocyte differentiation and upregulated in numerous types of solid tumors such as colorectal cancer (7), gastric cancer (8), and breast cancer (9). AEBP1 consists of an N-terminal discoidin-like domain, a carboxypeptidase domain, and a C-terminal DNA-binding domain (10). AEBP1 is found equally distributed both in the nucleus and cytoplasm and can change signal transduction through protein interaction in the cytoplasm and by transcriptionally regulating inflammatory and apoptotic genes in the nucleus (11).

AEBP1 was revealed to be significantly expressed in human gastric cancer tissues and gastric cancer cells, and silencing of AEBP1 inhibited the proliferation, migration and invasion of gastric cancer cells (12). Furthermore, AEBP1 knockdown could also inhibit tumor growth *in vivo* as confirmed by a xenograft mouse model. Mechanistically, knockdown of AEBP1 inhibited the downstream molecules of the NF- κ B/p65 pathway, which participate in the growth and metastasis of tumors (12). The Oncomine database revealed that AEBP1 is highly expressed in glioblastoma, and the further analysis of results showed that the high expression AEBP1 is associated with the poor prognosis of glioblastoma,

Correspondence to: Dr Cunfeng Jia, Department of Spinal Surgery, Zhangqiu District People's Hospital, 1920 Huiquan Road, Jinan, Shandong 250200, P.R. China
E-mail: zqqrmyjzkw@163.com

Key words: adipocyte enhancer-binding protein 1, proliferation, apoptosis, osteosarcoma

which indicated that AEBP1 could be a potential target for the development of novel therapies of glioblastoma (13). A novel treatment targeting glioma stem-like cells identified ACT001 as a regulator of the AEBP1 and AKT signaling pathways, which may suppress the growth of glioma stem-like cells and inhibit glioma sphere formation. Furthermore, AKT pathway activation could rescue the inhibition of cell proliferation induced by AEBP1 knockdown (14). The expression of AEBP1 was also observed in colorectal cancer tissues, and analysis of the clinical data revealed that the patients with high AEBP1 expression exhibited poor prognosis of colorectal cancer (15). Using miR-214 to downregulate the expression of AEBP1, Li *et al.* (15) found that AEBP1 depletion could inhibit the proliferation and promote the apoptosis of colorectal cancer cell lines. AEBP1 was revealed to be upregulated in breast cancer tissues compared with adjacent noncancerous tissues, and overexpression of AEBP1 promoted proliferation and metastasis through the activation of the ERK and AKT pathways and inhibited apoptosis by blocking cleavage of caspase-9 (9).

In the present study, AEBP1 was identified as a potential therapeutic target for OS. However, the molecular mechanism by which AEBP1 regulates OS has not been reported to date. Therefore, further exploration of the role of AEBP1 in OS proliferation is necessary to identify novel molecular targets.

Materials and methods

Extraction of data. A total of three expression profile datasets [GSE16088 (16), GSE197158 (17) and GSE63631 (18)] were selected and downloaded from the GEO database (<https://www.ncbi.nlm.nih.gov>) for analysis. Differentially expressed genes (DEGs) were analyzed by GEO2R (19). The screening conditions were as follows: Log₂-fold change <-1.5 or >1.5, and an adjusted P-value (adj. P) <0.05. The Venn diagram was constructed using Xiantao tool (<https://www.xiantaozi.com>), a web analysis tool. Data on AEBP1 expression from the Cancer Genome Atlas (TCGA) (<https://www.cancer.gov/tcga>) were extracted and analyzed using the UALCAN platform (<https://ualcan.path.uab.edu>) (20). Additionally, the expression of AEBP1 was analyzed using the Cancer Cell Line Encyclopedia (CCLE) (<https://sites.broadinstitute.org/ccle>).

Cell line and cell culture. Two OS cell lines (U2OS and HOS) were acquired from the Cell Bank of the Chinese Academy of Sciences (Shanghai, China). Briefly, the cells were maintained in Dulbecco's modified Eagle's medium supplemented with 10% fetal bovine serum (both from Gibco; Thermo Fisher Scientific, Inc.), 100 U/ml penicillin, and 100 µg/ml streptomycin at 37°C in a humidified atmosphere containing 5% CO₂.

siRNA and cell transfection. siRNAs targeting the AEBP1 sequence (sense, 5'-GGUGGUGGCUCGUUUAUC-3' and antisense, 5'-GAUGAAACGAGCCACCACC-3') and non-silencing sequences (sense, 5'-UUCUCCGAACGU GUCACGUTT-3' and antisense, 5'-GUGACACGUUCG GAGAATT-3') were procured from Guangzhou RiboBio Co., Ltd. Transfection with siRNAs was carried out using Lipofectamine 2000 transfection reagent (Thermo Fisher Scientific, Inc.) following the manufacturer's instructions.

Briefly, 100 pmol siRNA and Lipofectamine 2000 were added in the medium without FBS and antibiotics. Following incubation for 20 min at room temperature, the mixture was added in a 6-well plate and the medium was replaced with complete medium after 4 h. The cells were harvested after 48 h for the further determination.

Reverse transcription-quantitative PCR (RT-qPCR). Total RNA was extracted from OS cell lines (U2OS and HOS) using TRIzol reagent (Invitrogen; Thermo Fisher Scientific, Inc.) following the manufacturer's protocol. The extracted RNA was then reversely transcribed into cDNA using the FastKing RT Kit (ref. no. GKR116; Tiangen Biotech Co., Ltd.). Subsequently, RT-qPCR was performed using the ChamQ Universal SYBR qPCR Master Mix Kit (Vazyme Biotech Co., Ltd.) on an Applied Biosystems 7500 Real-time PCR System (Applied Biosystems, Inc.; Thermo Fisher Scientific, Inc.). Briefly, after an initial denaturation step at 95°C for 30 sec, the amplifications were carried out with 40 cycles at a melting temperature of 95°C for 10 sec and an annealing temperature of 60°C for 30 sec; followed by a melting curve analysis at 95°C for 15 sec, 60°C for 1 min, and 95°C for 15 sec. The following primers were used to detect the expression of AEBP1: Forward, 5'-ATGGAC TATTACTTTGGGCC-3' and reverse, 5'-GGGTAGTCC TCCTGGTGTCC-3'. β-actin was selected as the reference gene, and its expression was detected using the following primers: Forward, 5'-GCGTGACATTAAGGAGAAGC-3' and reverse, 5'-CCACGTCACACTTCATGATGG-3'. The relative gene expression was determined using the comparative Cq method (21), and each experiment was repeated at least three times.

Western blot analysis. Cells (U2OS and HOS) were harvested, and total protein was extracted using RIPA buffer supplemented with fresh protease and phosphatase inhibitors (Beyotime Institute of Biotechnology) following the manufacturer's instructions. The protein concentration was determined using a BCA assay (Nanjing KeyGen Biotech Co., Ltd.). Equal amounts of proteins (40 µg) were subjected to SDS-PAGE using 10% gels and transferred onto PVDF membranes. The membranes were blocked with 3% BSA (cat. no. KGL2314-10; Nanjing KeyGen Biotech Co., Ltd.) in 10 mM Tris-HCl (pH 7.4, with 0.05% Tween-20) for 1 h at room temperature and then incubated with primary antibodies at 4°C for 12 h. After washing with Tris-HCl buffer three times, the membranes were incubated with the corresponding peroxidase-conjugated secondary antibody (Abcam) at room temperature for 1 h. After washing with Tris-HCl buffer three times again, the protein bands were visualized using Super-Signal West Pico Chemiluminescent Substrate (Pierce; Thermo Fisher Scientific, Inc.), and their densitometry was quantified using ImageJ v1.8.0.345 software (National Institutes of Health). The detailed information regarding the antibodies is presented in Table SI. Each experiment was repeated at least three times.

MTT assay. OS (U2OS and HOS) cells (5,000 cells per well) were seeded in a 96-well plate in triplicate and cultured in a complete medium at 37°C for 1-5 days. Following

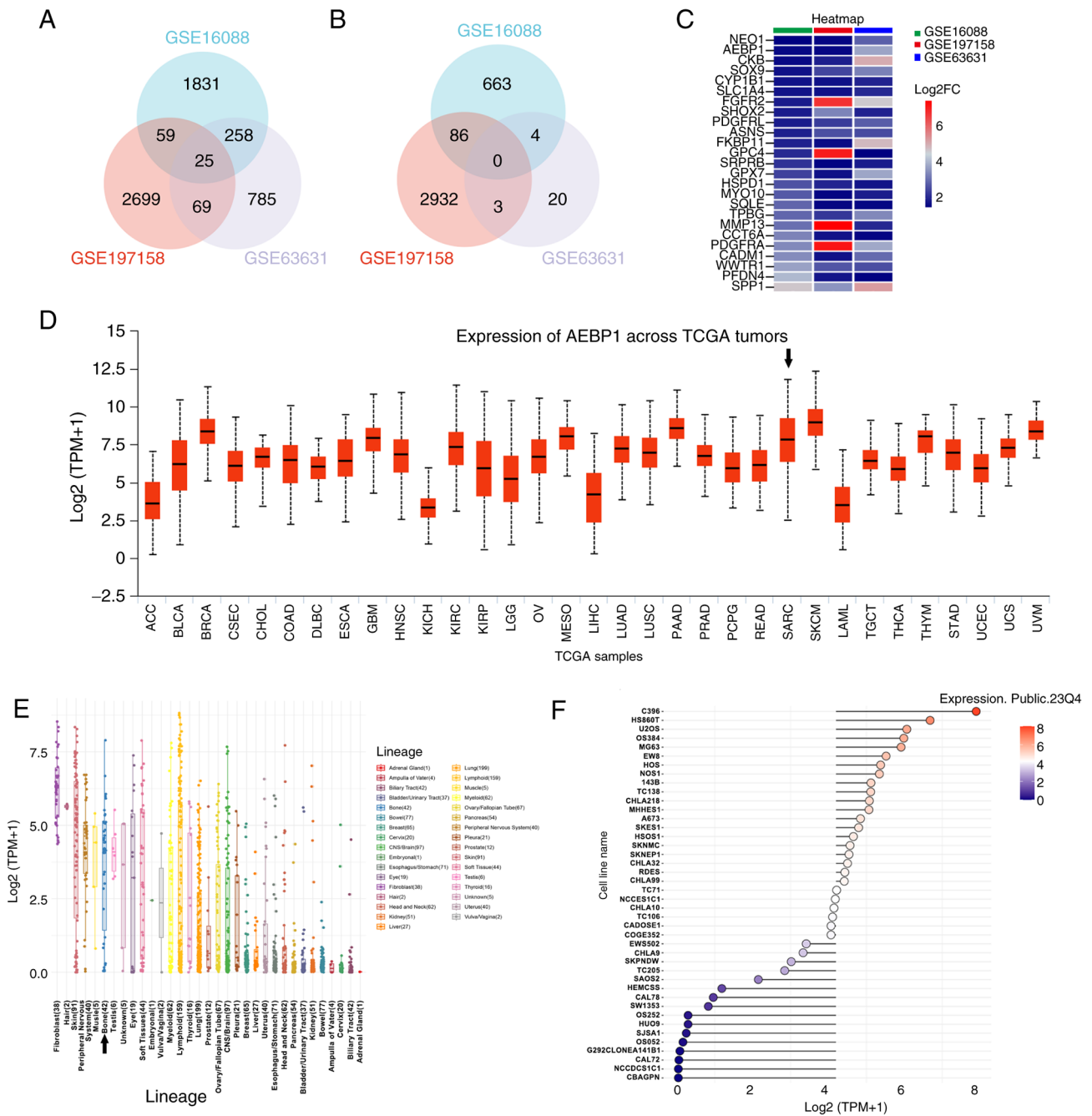


Figure 1. AEBP1 is a novel target for osteosarcoma and is markedly expressed in sarcoma and bone cancer cell lines. (A) Upregulated genes in 3 datasets (GSE16088, GSE197158 and GSE63631). (B) Downregulated genes in 3 datasets (GSE16088, GSE197158 and GSE63631). (C) The fold change of 25 upregulated genes of 3 datasets (GSE16088, GSE197158 and GSE63631). (D) Expression of AEBP1 across TCGA tumors. The black arrow indicates sarcoma. (E) Expression of AEBP1 in 33 types of cancer cell lines. The black arrow indicates bone cancer cell lines. (F) Expression of AEBP1 in bone cancer cell lines. Adipocyte enhancer-binding protein 1; TCGA, The Cancer Genome Atlas; ACC, adrenocortical carcinoma; BLCA, bladder urothelial carcinoma; BRCA, breast invasive carcinoma; CESC, cervical squamous cell carcinoma and endocervical adenocarcinoma; CHOL, cholangiocarcinoma; COAD, colon adenocarcinoma; DLBC, lymphoid neoplasm diffuse large B-cell lymphoma; ESCA, esophageal carcinoma; GBM, glioblastoma multiforme; HNSC, head and neck squamous cell carcinoma; KICH, kidney chromophobe; KIRC, kidney renal clear cell carcinoma; KIRP, kidney renal papillary cell carcinoma; LGG, brain lower grade glioma; OV, ovarian serous cystadenocarcinoma; MESO, mesothelioma; LIHC, liver hepatocellular carcinoma; LUAD, lung adenocarcinoma; LUSC, lung squamous cell carcinoma; PAAD, pancreatic adenocarcinoma; PRAD, prostate adenocarcinoma; PCPG, pheochromocytoma and paraganglioma; READ, rectum adenocarcinoma; SARC, sarcoma; SKCM, skin cutaneous melanoma; LAML, acute myeloid leukemia; TGCT, testicular germ cell tumors; THCA, thyroid carcinoma; THYM, thymoma; STAD, stomach adenocarcinoma; UCEC, uterine corpus endometrial carcinoma; UCS, uterine carcinosarcoma; UVM, uveal melanoma.

incubation, 100 μ l of MTT (cat. no. ST316; Beyotime Institute of Biotechnology) solution (5 mg/ml) was added to each well, and the plate was further incubated at 37°C for 4 h. Following incubation, the supernatant was carefully removed, and 150 μ l of DMSO was added to each well. The plate was

then oscillated for 30 min at room temperature to dissolve the formazan crystals. The absorbance at 490 nm was measured using a microplate reader, and the values were determined after subtracting the background. Each experiment was conducted at least three times.

Plate colony formation assay. Briefly, 400 cells (U2OS and HOS) were seeded in each well of a 6-well plate for the colony formation assay. After 2 weeks of incubation, the cells were washed three times with cold PBS at room temperature. Subsequently, the cells were fixed with 4% paraformaldehyde for 30 min at room temperature, followed by three washes with PBS. The cells were then stained with crystal violet dye for 20 min at room temperature. After staining, cell colonies were observed and imaged using a digital camera (Canon DS126211; Canon, Inc.). The plates were washed with distilled water before imaging. Colonies were defined as >50 cells and counted manually.

5-Ethynyl-2'-deoxyuridine (EdU) assay. The cell proliferation rate of U2OS and HOS cells was determined using the EdU incorporation assay following the manufacturer's instructions (BeyoClick™ EdU-555 EdU Kit; cat. no. C0075S; Beyotime Institute of Biotechnology). Images were captured under a fluorescence microscope (Leica Microsystems GmbH) from five randomly selected areas of each group. The EdU incorporation experiments were repeated at least three times to ensure the reliability and reproducibility of the results.

Flow cytometry (FCM). Cells (U2OS and HOS) were harvested, washed twice with cold PBS, and then fixed with cold 70% ethanol overnight at 4°C. After fixation, the cells were resuspended in PBS and stained with propidium iodide (PI) for 30 min at room temperature or Annexin V-APC (eBioscience, Inc.) for 30 min at room temperature. Subsequently, the stained cells were analyzed using a BD FACSCalibur flow cytometer (BD Biosciences). FlowJo software (v10.0; TreeStar) was used to analyze the data. This experiment was repeated at least three times to ensure the reliability of the results.

Terminal deoxynucleotidyl transferase-mediated dUTP nick-end labeling (TUNEL) assay. Cell apoptosis analysis was conducted using a TUNEL assay kit (cat. no. KGA1407-20; Nanjing KeyGen Biotech Co., Ltd.) following the manufacturer's instructions. Briefly, the cells were fixed using 4% paraformaldehyde for 30 min at room temperature, and then incubated with 0.2% Triton X-100 for 15 min at room temperature. The cells were washed three times using PBS solution for 5 min at room temperature. The cells were then incubated with TUNEL reagent for 30 min at 37°C. Finally, the nuclei were stained with DAPI (5 μg/ml) for 10 min at room temperature and the cells were mounted using an antifade mounting medium. A total of five fields were then observed under a fluorescence microscope (Leica Microsystems GmbH). This experiment was repeated at least three times to ensure the reliability of the results.

Rescue experiment. U2OS cells (20,000 cells per well) were seeded in a 6-well plate in triplicate and cultured in complete medium at 37°C. Following siRNA transfection for 48 h, an AKT pathway activator, 4 μg/ml SC79 (cat. no. S7863; Selleck Chemicals), was added in the medium. The cells were then cultured for 24 h at 37°C and harvested for further western blot analysis.

Statistical analysis. Statistical analysis was conducted using IBM SPSS Statistics software version 20 (IBM Corp.). Data

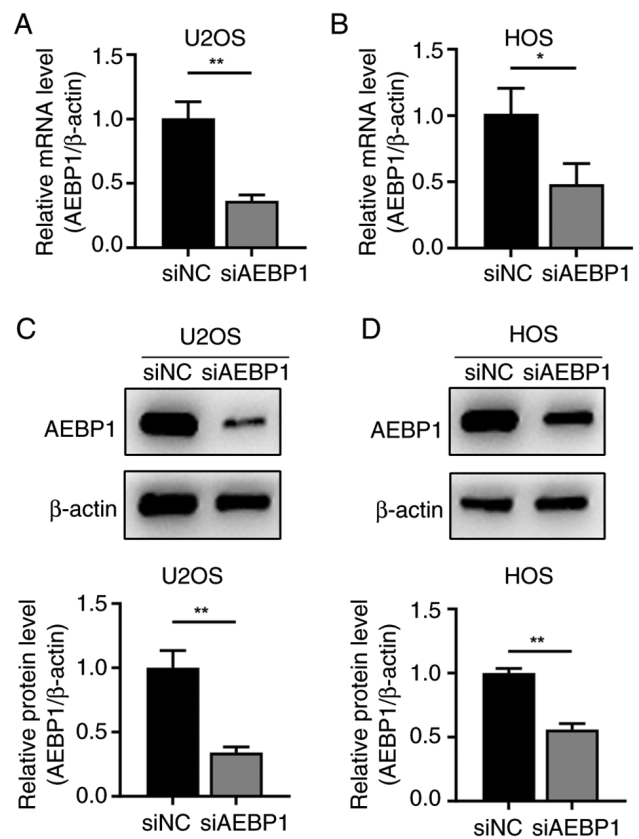


Figure 2. mRNA and protein level determination of AEBP1 in OS cell lines after AEBP1 knockdown. (A and B) The mRNA level of AEBP1 was examined by reverse transcription-quantitative PCR in U2OS and HOS cells, and β-actin was used as an internal control. (C and D) The protein level of AEBP1 was examined by western blot analysis, and β-actin was used as an internal control. *P<0.05 and **P<0.01. AEBP1, adipocyte enhancer-binding protein 1; OS, osteosarcoma; siNC, negative control group, siAEBP1, AEBP1-knockdown group.

were derived from a minimum of three independent experiments and are presented as the mean ± standard deviation. Unpaired Student's t-test was used for two-group comparisons and one-way analysis of variance (ANOVA) analysis was used for comparisons among multiple groups followed by Tukey's post hoc test. P<0.05 was considered to indicate a statistically significant difference.

Results

AEBP1 is identified as a novel target for osteosarcoma and markedly expressed in sarcoma tissues and OS cell lines. In order to screen the new molecular target for osteosarcoma, three GEO profiles were analyzed. GSE16088 contained human osteosarcoma tissues and normal tissues. GSE197158 contained osteosarcoma cell lines and normal osteoblast cell lines. GSE63631 contained mice osteosarcoma and normal tissues. Following GEO2R analysis and Venn diagram construction, 25 genes were identified to be upregulated in all the three datasets (Fig. 1A). In addition, there were no genes identified to be downregulated in all the three datasets (Fig. 1B). The fold change value is presented in Fig. 1C. There was one gene that was identified to be upregulated, AEBP1, and to the best of our knowledge, no studies on the association

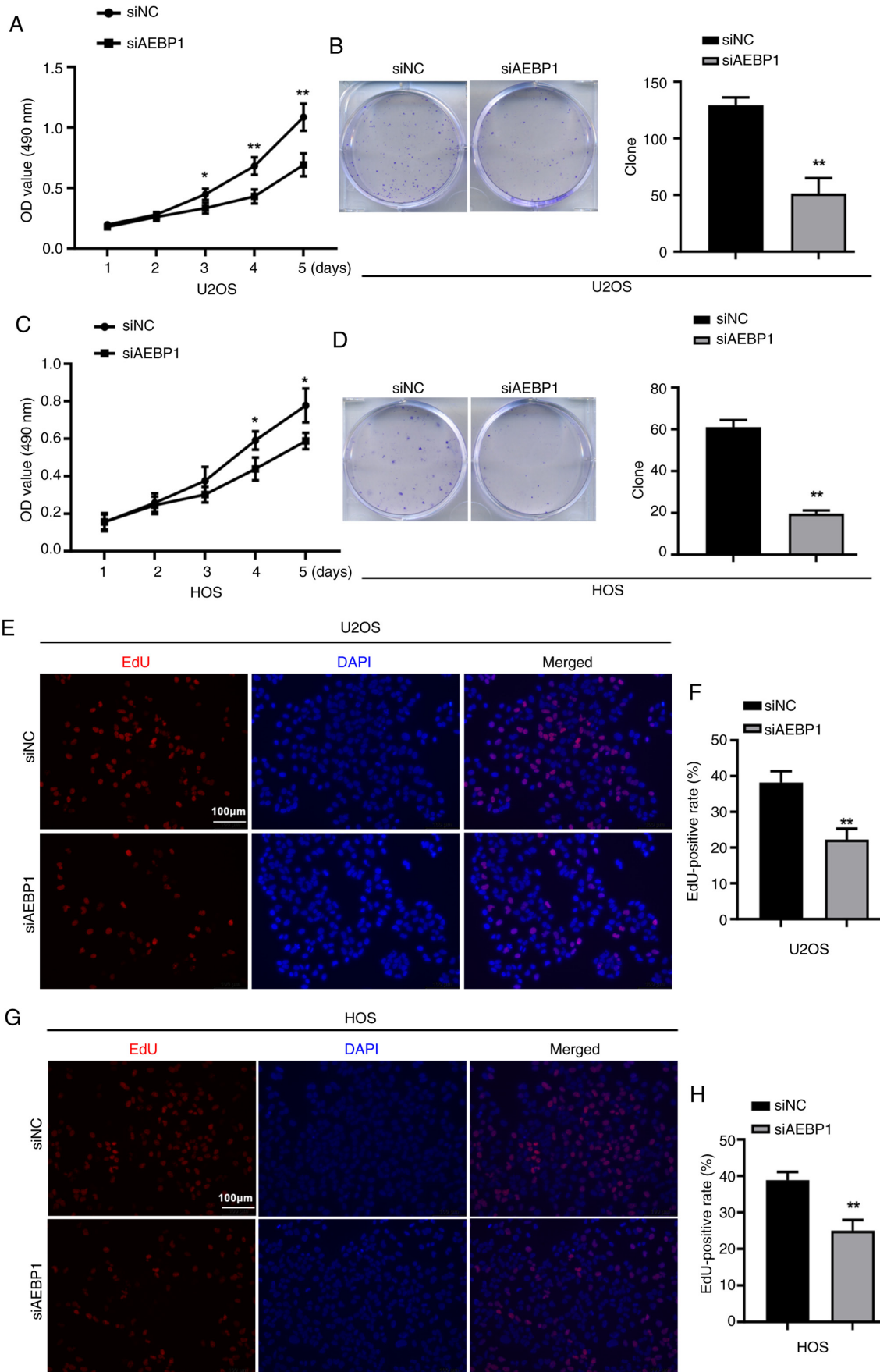


Figure 3. Effect of silencing of AEBP1 on OS cell proliferation. An MTT assay was used to determine the proliferation of siAEBP1 and the negative control in (A) U2OS and (B) HOS cells for 5 days. Cell clones of siAEBP1-treated cells and negative control cells in (C) U2OS and (D) HOS cells were observed by clone formation assay. An EdU assay was performed in (E) U2OS and (G) HOS cells. Analysis of the results of the EdU assay in (F) U2OS and (H) in HOS cells. Scale bar, 100 μm. *P<0.05 and **P<0.01. AEBP1, adipocyte enhancer-binding protein 1; OS, osteosarcoma; siAEBP1, AEBP1-knockdown group; siNC, negative control group; EdU, 5-ethynyl-2'-deoxyuridine.

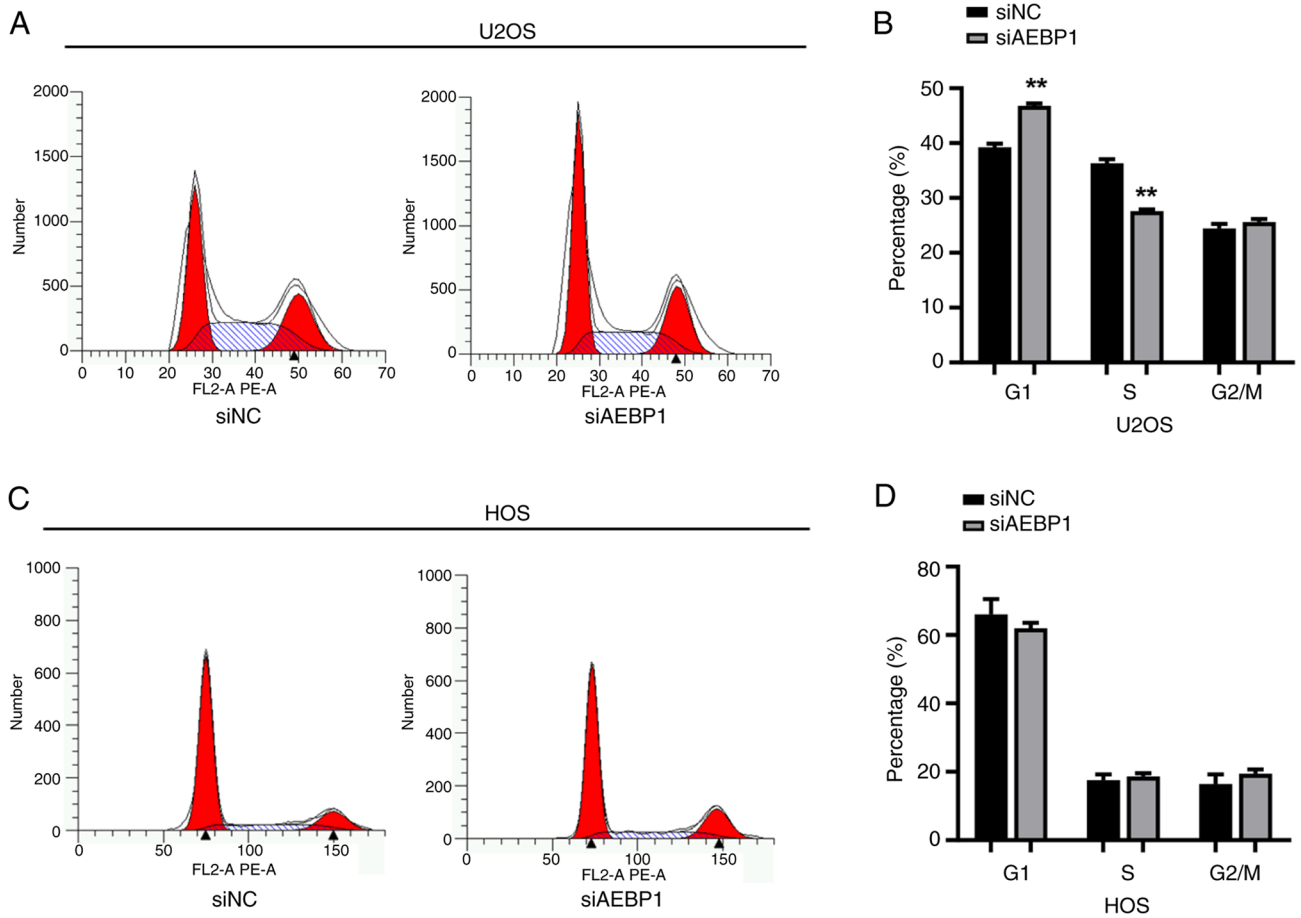


Figure 4. Effect of AEBP1-knockdown on the OS cell cycle. The percentage of siAEBP1-treated cells and negative control cells in the different phases of the cell cycle was determined and analyzed by flow cytometry in (A and B) U2OS and (C and D) HOS cells. ** $P < 0.01$. AEBP1, adipocyte enhancer-binding protein 1; OS, osteosarcoma; siAEBP1, AEBP1-knockdown group; siNC, negative control group.

between this gene and osteosarcoma have been reported to date. To explore the relationship between AEBP1 expression and tumors, an analysis using datasets from TCGA, available on the UALCAN database was conducted. The TCGA database includes sarcoma data but does not distinctly categorize osteosarcoma from other sarcoma subtypes. The findings revealed a high expression of AEBP1 (ranked 8th among all 33 types of tumors) in sarcoma tissue compared with other tumor tissues (Fig. 1D). Although sarcoma also includes tumors originating from muscle and adipose tissue, the results suggested that AEBP1 may be associated with osteosarcoma. Furthermore, the expression of AEBP1 was analyzed in cancer cell lines using the CCLE database and markedly high expression was identified in bone cancer cell lines (Fig. 1E and F). Based on these findings, two OS cell lines, U2OS and HOS were selected for further research on AEBP1 expression in OS.

Silencing of AEBP1 increases the cytotoxicity and inhibits the proliferation of human OS cells. To investigate the role of AEBP1 in regulating OS, AEBP1 was silenced by transfecting siRNA targeting AEBP1 into OS cells. Following siRNA transfection, the expression of AEBP1 at the both mRNA and protein levels was significantly decreased in U2OS and HOS cells (Fig. 2A-D).

The effect of AEBP1 silencing on cell proliferation was then examined using MTT, colony formation assays, and EdU assays. The results of MTT assays revealed that silencing of AEBP1 increased the cytotoxicity of OS cells (Fig. 3A and C). Additionally, the formation of cell colonies was significantly inhibited after silencing of AEBP1, with the number of colonies decreasing by 60.5% in U2OS cells and 67.2% in HOS cells (Fig. 3B and D).

The EdU assay further indicated a significant decrease in proliferation following silencing of AEBP1. The number of EdU-positive cells was significantly reduced in AEBP1-silenced cells compared with control cells, with U2OS cells showing a decrease from 38.2 to 22.3% and HOS cells showing a decrease from 38.8 to 25.0% (Fig. 3E-H).

Silencing of AEBP1 induces G₁ cell cycle arrest in human OS U2OS cells. To elucidate how AEBP1 regulated cell growth, FCM was used to analyze the cell cycle. In U2OS cells, the results showed that the percentage of cells in the G₁ phase was 39.2% in the control group and increased to 46.8% in the AEBP1-silenced group. Conversely, the percentage of cells in the S phase decreased from 36.3% in the control group to 27.6% in the AEBP1-silenced group (Fig. 4A and B). These findings indicated that knockdown of AEBP1 induced G₁ phase arrest in U2OS cells. However, a consistent trend was

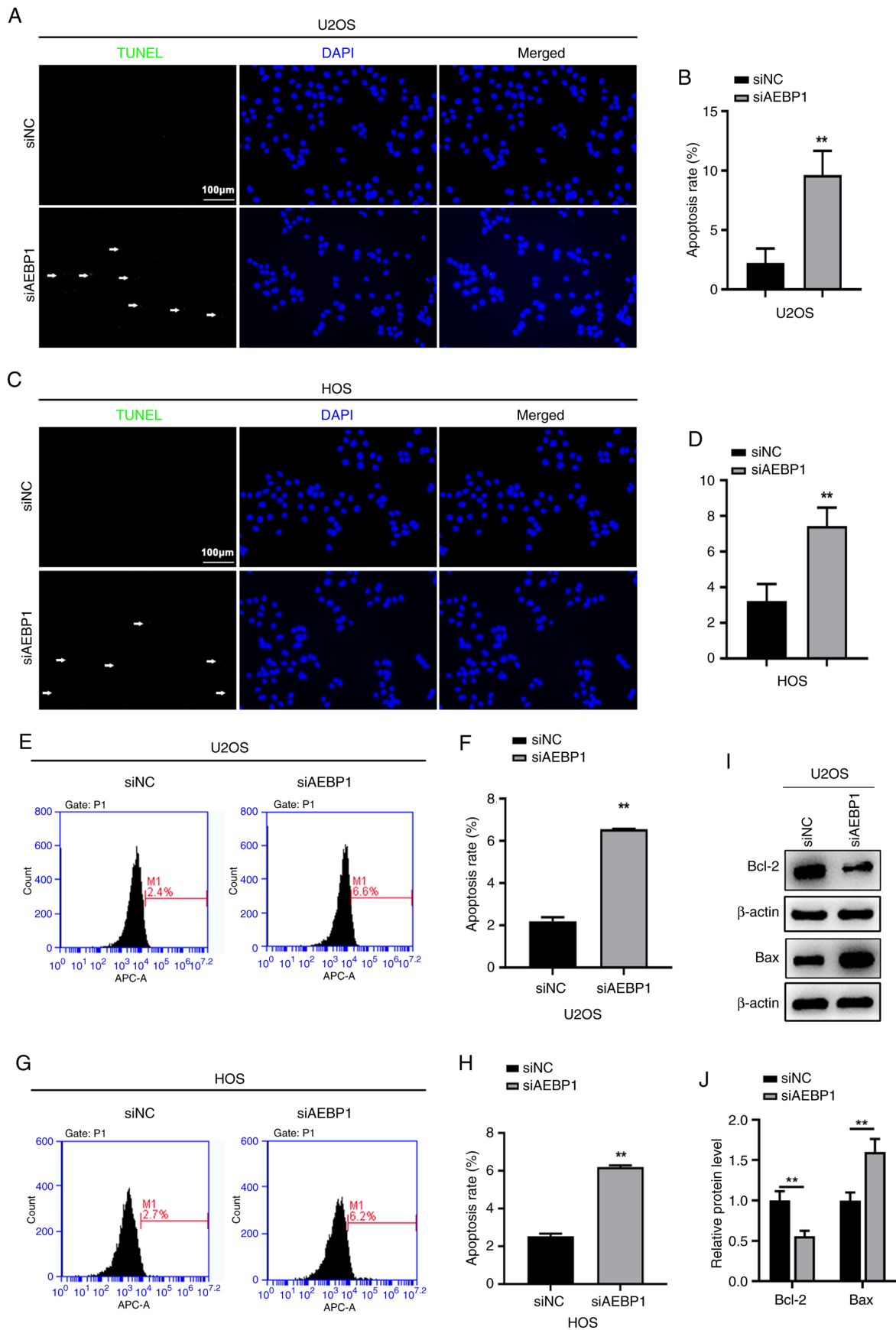


Figure 5. AEBP1 knockdown promotes the apoptosis of OS cells. (A-D) A TUNEL assay revealed that apoptosis was increased after AEBP1 knockdown in (A and B) U2OS cells and (C and D) HOS cells. (E-H) Flow cytometry demonstrated that apoptosis was increased after AEBP1 knockdown in (E and F) U2OS cells and (G and H) HOS cells. The white arrows indicate the TUNEL-positive cells. (I) The protein expression level of Bcl-2 was downregulated and that of Bax was upregulated after AEBP1 knockdown in U2OS cells. (J) Statistical analysis of I. Scale bar, 100 μ m. ** P <0.01. AEBP1, adipocyte enhancer-binding protein 1; OS, osteosarcoma; siAEBP1, AEBP1-knockdown group; siNC, negative control group; TUNEL, terminal deoxynucleotidyl transferase-mediated dUTP nick-end labeling.

not observed in HOS cells. Following silencing of AEBP1, there was no significant change in the cell cycle of HOS cells (Fig. 4C and D).

Silencing of AEBP1 promotes apoptosis in human OS cells. To investigate the role of AEBP1 in regulating the proliferation of OS cells, the changes in apoptosis were evaluated, following AEBP1 silencing, using TUNEL and FCM assays. TUNEL staining revealed a significant increase in the percentage of TUNEL-positive cells in both U2OS and HOS cells following silencing of AEBP1. In U2OS cells, the percentage of TUNEL-positive cells increased from 2.2% in control cells to 9.6% in AEBP1-silenced cells (Fig. 5A and B). Similarly, in HOS cells, the percentage of TUNEL-positive cells increased from 3.2% in control cells to 7.4% after silencing of AEBP1 (Fig. 5C and D). Consistent with these findings, the results of FCM showed a significant increase in the apoptotic rate of U2OS cells after silencing of AEBP1 (6.6%) compared with control cells (2.2%) (Fig. 5E and F). Similarly, the apoptotic rate of HOS cells significantly increased after AEBP1 knockdown (6.2%) compared with control cells (2.5%) (Fig. 5G and H). Considering that silencing of AEBP1 promoted apoptosis, the levels of Bcl-2 and Bax, key regulators of apoptosis, were also assessed. The findings revealed downregulation of Bcl-2 and upregulation of Bax following silencing of AEBP1 (Fig. 5I and J).

Silencing of AEBP1 inhibits cell proliferation through the AKT signaling pathway. To elucidate the mechanism underlying AEBP1-induced proliferation and apoptosis, the AKT signaling pathway, a regulator of cell proliferation and apoptosis (22), was investigated in U2OS cells. The results demonstrated that phosphorylated AKT (p-AKT) levels significantly decreased following AEBP1 silencing, while total AKT levels remained unchanged (Fig. 6A and C). Furthermore, since silencing of AEBP1 induced G₁ phase arrest in U2OS cells, the protein expression level of cyclin D1, a key regulator of the G₁ phase of the cell cycle and a downstream factor of the AKT signaling pathway (23), was examined. The results showed a decrease in the protein level of cyclin D1 following silencing of AEBP1 (Fig. 6A and C).

To further validate the involvement of the AKT signaling pathway, rescue experiments were performed by adding an AKT pathway activator (SC79). It was revealed that SC79 significantly rescued the inhibitory effect induced by AEBP1 silencing (Fig. 6B and D). In conclusion, the data indicated that AEBP1 regulated the proliferation of OS cells primarily through the AKT signaling pathway.

Discussion

In the present study, AEBP1 was initially identified as a novel target for osteosarcoma and high expression of AEBP1 was observed in human sarcoma tissues and OS cell lines. Subsequently, the role of AEBP1 in regulating the proliferation of OS cells through the AKT signaling pathway was explored. The AKT signaling pathway plays a crucial role in cell growth and survival, protein synthesis, and glucose metabolism (24). Dysregulation of this pathway is observed in various tumor types, leading to investigations

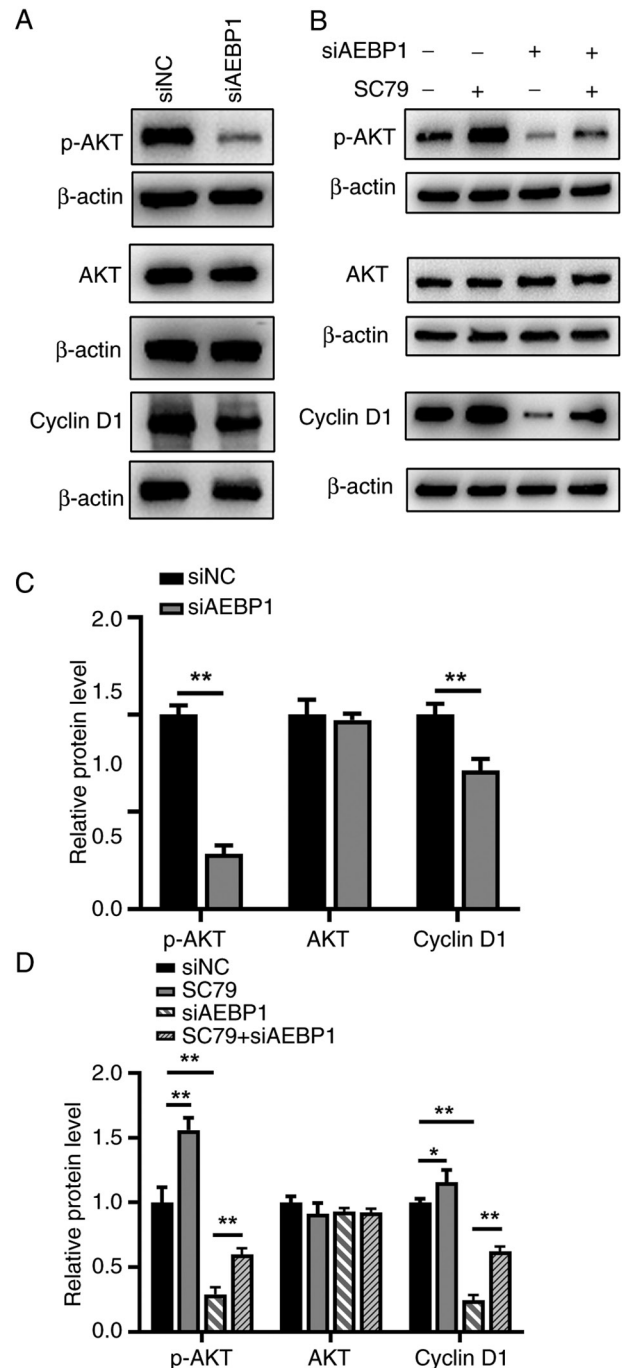


Figure 6. Regulatory mechanism of AEBP1 in the proliferation of OS. Western blot analysis was carried out to detect the expression of cell cycle checkpoint proteins in U2OS cells. (A) The protein expression level of p-AKT (the phosphate site was Thr308) was downregulated while the expression level of total AKT was not altered after AEBP1 knockdown. In addition, the protein expression level of cyclin D1 was decreased after AEBP1 knockdown. (B) The protein expression level of p-AKT was upregulated after the addition of SC79, a stimulator of the AKT signaling pathway. SC79 could rescue the inhibitory effect induced by AEBP1 knockdown. (C) Statistical analysis of A. ** $P < 0.01$ vs. the corresponding group indicated. (D) The statistical analysis of B. * $P < 0.05$ and ** $P < 0.01$ vs. the corresponding group indicated. AEBP1, adipocyte enhancer-binding protein 1; OS, osteosarcoma; siAEBP1, AEBP1-knockdown group; siNC, negative control group; p-, phosphorylated.

into its inhibition in different cancer models, including the triple-negative subtype of breast cancer (25). During the progression of mammary gland tumorigenesis, AEBP1

could enhance the activity of NF- κ B/p65 and Akt mediated by TNF- α secretion, and transplantation of AEBP1 in bone marrow cells may lead to alveolar hyperplasia contributing to upregulation of NF- κ B activity and TNF- α expression (26). Western blotting analysis further supported the hypothesis that AEBP1 regulated OS growth through the AKT signaling pathway. The additional experiments, wherein an activator of the AKT pathway was able to rescue the inhibition induced by silencing of AEBP1, further confirmed the conclusion.

Cyclin D1 is a key mediator of AKT in regulating cell proliferation. Phosphorylation of cyclin D1 at Thr286 by glycogen synthase kinase 3 β (GSK3 β) leads to its ubiquitin-mediated degradation (27). AKT-dependent phosphorylation inhibits GSK3 β catalytic activity, thereby stabilizing cyclin D1. Additionally, AKT can regulate cyclin D1 expression through the NF- κ B/I κ B kinase pathway (28). Cell cycle progression in all eukaryotes is tightly regulated by an intricate mechanism involving cyclin-dependent kinases (CDKs) binding with the corresponding cyclin regulatory subunits in a sequential manner. The G₁ phase cyclins, cyclin D, and cyclin E, predominantly associate with CDK4/CDK6 and CDK2 to promote G₁ progression and entry into the S phase (29). In the present study, it was observed that silencing of AEBP1 induced G₁ phase arrest in U2OS cells and inhibited cell proliferation.

It was also further explored whether AEBP1 could influence the apoptosis of OS cells. Li *et al* (30) reported that AEBP1 knockdown could markedly promote the apoptosis of Jurkat cells via the p53/Bcl-2 pathway, indicated that AEBP1 may be pivotal to apoptosis (30). The Bcl-2 family plays a critical role in determining cell fate. In mammalian cells, the intrinsic mitochondrial pathway of apoptosis is tightly regulated by Bcl-2 family proteins, including Bcl-2, Bcl-XL, and MCL-1 (31). While Bcl-2 is an anti-apoptotic protein, Bax is a pro-apoptotic effector protein. Inhibition of Bcl-2 has previously been shown to promote apoptosis in leukemic cells (32). The results of the present study indicated that silencing of AEBP1 promoted apoptosis by inhibiting Bcl-2 and upregulating Bax.

In conclusion, it was demonstrated that AEBP1 regulated the proliferation of OS primarily through the AKT signaling pathway, affecting both cell proliferation and apoptosis. Therefore, AEBP1 may serve as a potential therapeutic target for treating OS.

Acknowledgements

Not applicable.

Funding

The present study was supported by the research fund of Science and Technology Plan of Jinan Health Commission (grant no. 2021-2-124).

Availability of data and materials

The data generated in the present study may be requested from the corresponding author.

Authors' contributions

CJ conceived and designed the study. ZG and LZ performed the bioinformatics analysis and statistical analysis. CJ conducted laboratory experiments. CJ, ZG and LZ wrote and revised the manuscript. CJ, ZG and LZ confirm the authenticity of all the raw data. All authors read and approved the final version of the manuscript.

Ethics approval and consent to participate

Not applicable.

Patient consent for publication

Not applicable.

Competing interests

The authors declare that they have no competing interests.

References

- Li Z, Li X, Xu D, Chen X, Li S, Zhang L, Chan MTV and Wu WKK: An update on the roles of circular RNAs in osteosarcoma. *Cell Prolif* 54: e12936, 2021.
- Mirabello L, Troisi RJ and Savage SA: Osteosarcoma incidence and survival rates from 1973 to 2004: Data from the surveillance, epidemiology, and end results program. *Cancer* 115: 1531-1543, 2009.
- Whelan J, McTiernan A, Cooper N, Wong YK, Francis M, Vernon S and Strauss SJ: Incidence and survival of malignant bone sarcomas in England 1979-2007. *Int J Cancer* 131: E508-E517, 2012.
- Sheng G, Gao Y, Yang Y and Wu H: Osteosarcoma and metastasis. *Front Oncol* 11: 780264, 2021.
- Chen C, Xie L, Ren T, Huang Y, Xu J and Guo W: Immunotherapy for osteosarcoma: Fundamental mechanism, rationale, and recent breakthroughs. *Cancer Lett* 500: 1-10, 2021.
- He GP, Muise A, Li AW and Ro HS: A eukaryotic transcriptional repressor with carboxypeptidase activity. *Nature* 378: 92-96, 1995.
- Sugai T, Yamada N, Osakabe M, Hashimoto M, Uesugi N, Eizuka M, Tanaka Y, Sugimoto R, Yanagawa N and Matsumoto T: Microenvironmental markers are correlated with lymph node metastasis in invasive submucosal colorectal cancer. *Histopathology* 79: 584-598, 2021.
- Li S, Liu X, Liu T, Meng X, Yin X, Fang C, Huang D, Cao Y, Weng H, Zeng X and Wang X: Identification of biomarkers correlated with the TNM staging and overall survival of patients with bladder cancer. *Front Physiol* 8: 947, 2017.
- Li J, Ruan Y, Zheng C, Pan Y, Lin B, Chen Q and Zheng Z: AEBP1 contributes to breast cancer progression by facilitating cell proliferation, migration, invasion, and blocking apoptosis. *Discov Med* 35: 45-56, 2023.
- Lyons PJ, Mattatall NR and Ro HS: Modeling and functional analysis of AEBP1, a transcriptional repressor. *Proteins* 63: 1069-1083, 2006.
- Ladha J, Sinha S, Bhat V, Donakonda S and Rao SMR: Identification of genomic targets of transcription factor AEBP1 and its role in survival of glioma cells. *Mol Cancer Res* 10: 1039-1051, 2012.
- Liu JY, Jiang L, Liu JJ, He T, Cui YH, Qian F and Yu PW: AEBP1 promotes epithelial-mesenchymal transition of gastric cancer cells by activating the NF- κ B pathway and predicts poor outcome of the patients. *Sci Rep* 8: 11955, 2018.
- Liu M, Yu Y, Zhang Z, Chen Z, Chen B, Cheng Y, Wei Y, Li J and Shang H: AEBP1 as a potential immune-related prognostic biomarker in glioblastoma: A bioinformatic analyses. *Ann Transl Med* 9: 1657, 2021.
- Hou Y, Sun B, Liu W, Yu B, Shi Q, Luo F, Bai Y and Feng H: Targeting of glioma stem-like cells with a parthenolide derivative ACT001 through inhibition of AEBP1/PI3K/AKT signaling. *Theranostics* 11: 555-566, 2021.

15. Li S, Li C and Fang Z: MicroRNA 214 inhibits adipocyte enhancer-binding protein 1 activity and increases the sensitivity of chemotherapy in colorectal cancer. *Oncol Lett* 17: 55-62, 2019.
16. Paoloni M, Davis S, Lana S, Withrow S, Sangiorgi L, Picci P, Hewitt S, Triche T, Meltzer P and Khanna C: Canine tumor cross-species genomics uncovers targets linked to osteosarcoma progression. *BMC Genomics* 10: 625, 2009.
17. Wood RK, Flory AR, Mann MJ, Talbot LJ and Hendershot LM: Secretory defects in pediatric osteosarcoma result from down-regulation of selective COPII coatomer proteins. *iScience* 25: 104100, 2022.
18. Sato S, Tang YJ, Wei Q, Hirata M, Weng A, Han I, Okawa A, Takeda S, Whetstone H, Nadesan P, *et al.*: Mesenchymal tumors can derive from Ng2/Cspg4-expressing pericytes with β -catenin modulating the neoplastic phenotype. *Cell Rep* 16: 917-927, 2016.
19. Barrett T, Wilhite SE, Ledoux P, Evangelista C, Kim IF, Tomashevsky M, Marshall KA, Phillippy KH, Sherman PM, Holko M, *et al.*: NCBI GEO: Archive for functional genomics data sets-update. *Nucleic Acids Res* 41: D991-D995, 2013.
20. Chandrashekar DS, Bashel B, Balasubramanya SAH, Creighton CJ, Ponce-Rodriguez I, Chakravarthi BVSK and Varambally S: UALCAN: A portal for facilitating tumor subgroup gene expression and survival analyses. *Neoplasia* 19: 649-658, 2017.
21. Livak KJ and Schmittgen TD: Analysis of relative gene expression data using real-time quantitative PCR and the 2(-Delta Delta C(T)) method. *Methods* 25: 402-408, 2001.
22. Dong M, Yang G, Liu H, Liu X, Lin S, Sun D and Wang Y: Aged black garlic extract inhibits HT29 colon cancer cell growth via the PI3K/Akt signaling pathway. *Biomed Rep* 2: 250-254, 2014.
23. Zhu Y, Wu F, Hu J, Xu Y, Zhang J, Li Y, Lin Y and Liu X: LDHA deficiency inhibits trophoblast proliferation via the PI3K/AKT/FOXO1/CyclinD1 signaling pathway in unexplained recurrent spontaneous abortion. *FASEB J* 37: e22744, 2023.
24. Mills JN, Rutkovsky AC and Giordano A: Mechanisms of resistance in estrogen receptor positive breast cancer: Overcoming resistance to tamoxifen/aromatase inhibitors. *Curr Opin Pharmacol* 41: 59-65, 2018.
25. Politz O, Siegel F, Bäracker L, Bömer U, Hägebarth A, Scott WJ, Michels M, Ince S, Neuhaus R, Meyer K, *et al.*: BAY 1125976, a selective allosteric AKT1/2 inhibitor, exhibits high efficacy on AKT signaling-dependent tumor growth in mouse models. *Int J Cancer* 140: 449-459, 2017.
26. Holloway RW, Bogachev O, Bharadwaj AG, McCluskey GD, Majdalawieh AF, Zhang L and Ro HS: Stromal adipocyte enhancer-binding protein (AEBP1) promotes mammary epithelial cell hyperplasia via proinflammatory and hedgehog signaling. *J Biol Chem* 287: 39171-39181, 2012.
27. Guo Y, Yang K, Harwalkar J, Nye JM, Mason DR, Garrett MD, Hitomi M and Stacey DW: Phosphorylation of cyclin D1 at Thr 286 during S phase leads to its proteasomal degradation and allows efficient DNA synthesis. *Oncogene* 24: 2599-2612, 2005.
28. Guo X, Li W, Wang Q and Yang HS: AKT activation by pcd4 knockdown up-regulates cyclin D1 expression and promotes cell proliferation. *Genes Cancer* 2: 818-828, 2011.
29. Wang Z, Wang Y, Wang S, Meng X, Song F, Huo W, Zhang S, Chang J, Li J, Zheng B, *et al.*: Coxsackievirus A6 induces cell cycle arrest in G0/G1 phase for viral production. *Front Cell Infect Microbiol* 8: 279, 2018.
30. Li S, Juan CX, Feng AM, Bian HL, Liu WD, Zhang GQ, Wang CZ, Cao Q and Zhou GP: Attenuating the abnormally high expression of AEBP1 suppresses the pathogenesis of childhood acute lymphoblastic leukemia via p53-dependent signaling pathway. *Eur Rev Med Pharmacol Sci* 23: 1184-1195, 2019.
31. Lin KN, Zhao W, Huang SY and Li H: Grape seed proanthocyanidin extract induces apoptosis of HL-60/ADR cells via the Bax/Bcl-2 caspase-3/9 signaling pathway. *Transl Cancer Res* 10: 3939-3947, 2021.
32. Choi JH, Bogenberger JM and Tibes R: Targeting apoptosis in acute myeloid leukemia: Current status and future directions of BCL-2 inhibition with venetoclax and beyond. *Target Oncol* 15: 147-162, 2020.



Copyright © 2025 Jia et al. This work is licensed under a Creative Commons Attribution-NonCommercial-NoDerivatives 4.0 International (CC BY-NC-ND 4.0) License.